ACS OMEGA

Article

Spatially Localized Synthesis and Structural Characterization of Platinum Nanocrystals Obtained Using UV Light

Jonathan Quinson,*[†,§] Laura Kacenauskaite,[†,§] Troels L. Christiansen,[†] Tom Vosch,*[†] Matthias Arenz,*[‡,†] and Kirsten M. Ø. Jensen*[†]

[†]Nano-Science Center, Department of Chemistry, University of Copenhagen, Universitetsparken 5, DK-2100 Copenhagen Ø, Denmark

[‡]Department of Chemistry and Biochemistry, University of Bern, Freiestrasse 3, CH-3012 Bern, Switzerland

S Supporting Information

ABSTRACT: Platinum nanocrystals with a fine control of the crystal domain size in the range 1.0−2.2 nm are produced by tuning the NaOH concentration during the UV-induced reduction of H_2PtCl_6 in surfactant-free alkaline ethylene glycol. The colloidal solutions obtained are characterized by transmission electron microscopy and pair distribution function analysis, allowing analysis of both atomic and nanoscale structures. The obtained nanoparticles exhibit a face-centered cubic crystal structure even for the smallest nanoparticles, and the cubic unit cell parameter is significantly reduced with decreasing crystallite size. It is further demonstrated how the "UV-approach" can be used to achieve spatial control of the nucleation and growth of the platinum nanocrystals, which is not possible by thermal reduction.
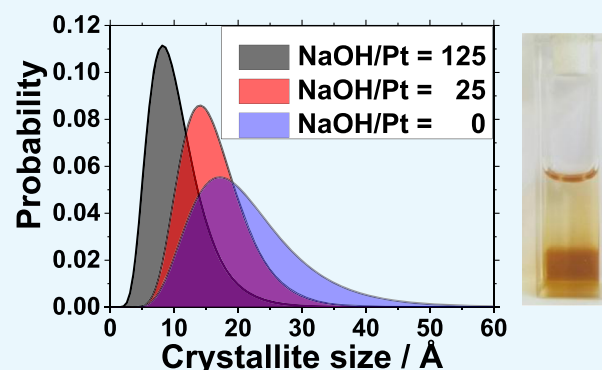
INTRODUCTION

To optimize catalysts for chemical production or energy applications, developing nanomaterials has proven to be a rewarding strategy. In particular, costly precious metal catalysts benefit from being scaled down to few nanometers since nanomaterials show high surface-to-volume ratios and only surface atoms are involved in catalytic processes. At the nanoscale, size and structure control are key:[1] nanoparticle catalyst properties like catalytic activity, selectivity, and/or stability[2] are strongly affected by their size and structure.[3] Since most of the catalytic properties relate to the specific atomic arrangements between precious metal atoms,[4,5] the structure of the nanoparticles should ideally be controlled and well defined even at the smallest nanoparticle size.

Assessing the crystal structure of materials of few or sub-nanometers can be challenging by standard techniques such as X-ray diffraction or high-resolution electron transmission microscopy (HRTEM).[6] Pair distribution function analysis (PDF) of X-ray total scattering data is here used along with transmission electron microscopy (TEM) to characterize the structure, size, and size distribution of Pt nanoparticles obtained by a recently introduced UV-induced synthesis in alkaline ethylene glycol (EG).[7] It is first confirmed that increasing the NaOH/Pt molar ratio leads to smaller nanoparticles[3] in the UV-induced synthesis. PDF analysis shows that the size distribution increases with crystallite size, and it is established that even the smallest nanoparticles take the face-centered cubic (fcc) crystal structure, where the unit cell parameter decreases with decreasing crystallite size.

Furthermore, it is demonstrated that UV-induced synthesis offers unique options for the localized synthesis of nanoparticles: a feature that could be relevant to the further development of nano-based devices where localized formation of nanoparticles is key.

RESULTS AND DISCUSSION

The ethylene glycol (EG) process is a popular green synthesis method to produce nanoparticles;[8,9] in particular, precious metal nanoparticles like platinum (Pt) can be obtained without using a surfactant.[10] The particle formation can be induced in different ways: at ambient temperature conditions,[11] using thermal synthesis,[10] using microwaves,[12] or using UV light, as we recently showed.[7] Due to its simplicity, the UV method is a promising alternative to standard thermal synthesis routes as only a UV-transparent container and a UV source are needed. Here, size control in the UV synthesis of Pt nanoparticles is achieved by tuning the concentration of NaOH.[7] In the present study, the NaOH/Pt molar ratio is changed from 125 to 0. TEM analysis in Figure 1 reveals that the particle size is then controlled in the range 1.9 (±0.5) to 3.4 (±0.6) nm.

One of the large obstacles in the characterization of the atomic structure of nanoparticles is that conventional diffraction methods, that is, powder X-ray diffraction with Rietveld refinement analysis, are challenged when going to the
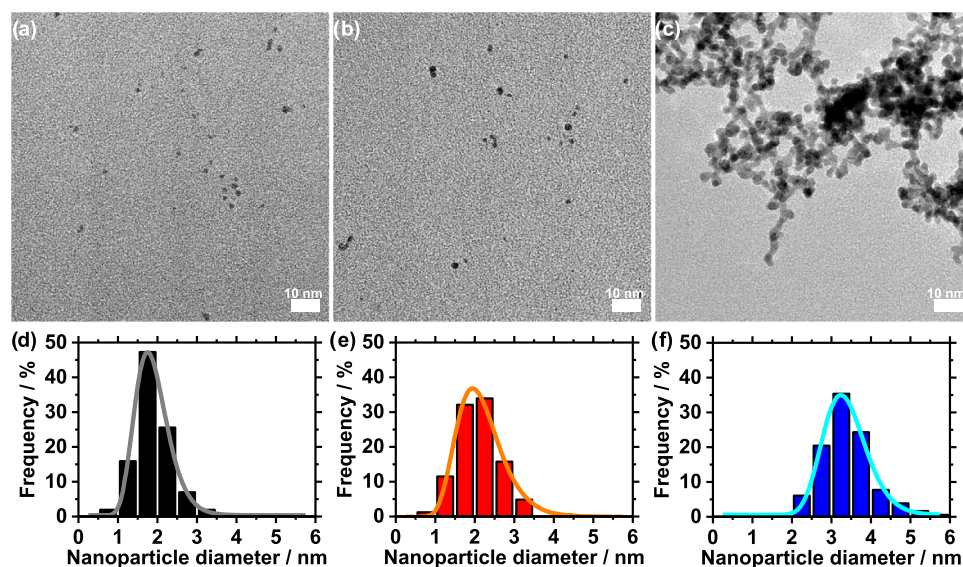
Figure 1. (a−c) TEM micrographs and (d−f) size distribution including log−normal fits for Pt nanoparticles obtained by NaOH/Pt molar ratios of: (a, d) 125, (b, e) 25, and (c, f) 0.

nanoscale: the lack of long-range order makes crystallographic methods insufficient. Bragg peaks broaden as the particles get smaller, and new structures different from those known from bulk chemistry may also become stable when going to the extreme nanoscale.[13−15] However, by using the X-ray total scattering signal (including both Bragg peaks and diffuse scattering) and pair distribution function (PDF) analysis, it is possible to characterize the structure of materials without long-range order.[6,16] Over the last decade, this technique has been demonstrated for the structural characterization of a large range of different nanoparticles,[17−19] including ultrasmall metallic nanoparticles[14,15] and platinum-based catalyst materials,[20−25] and has helped in understanding how new structural motifs become stable when going to nanosized materials. Compared to HRTEM, where structural information is obtained at the expense of time-consuming and often challenging imaging of several individual single nanoparticles, PDF analysis provides the average structure of a sample of nanomaterials.

Here, PDF is performed to investigate the effect of a change in the initial NaOH/Pt molar ratio on the nanoparticle size and structure. The X-ray total scattering data obtained for suspensions of Pt nanoparticles in EG prepared with different NaOH/Pt ratios are shown in Figure 2a. The large majority of the signal arises from the EG solvent, as can be seen when comparing the measurement from the pure EG with the nanoparticle-containing samples. Clear Bragg peaks are seen from the particles obtained with the lowest NaOH/Pt molar ratios, while broader, weaker features are seen in the scattering pattern for the particles prepared with NaOH/Pt = 25 and 125.

The PDFs obtained from the data are shown in Figure 2b. The data clearly show that the ordered domain size increases with decreasing NaOH/Pt molar ratio as PDF peaks extend to higher r-values as the NaOH/Pt molar ratio is decreased. For the Pt nanoparticles studied here, control of the crystallite size in the range 2.2−1.0 nm is achieved by changing the NaOH/Pt molar ratio from 0 to 125.

To extract quantitative information, the PDFs were modeled using Diffpy-CMI.[26] The PDFs were modeled applying the fcc
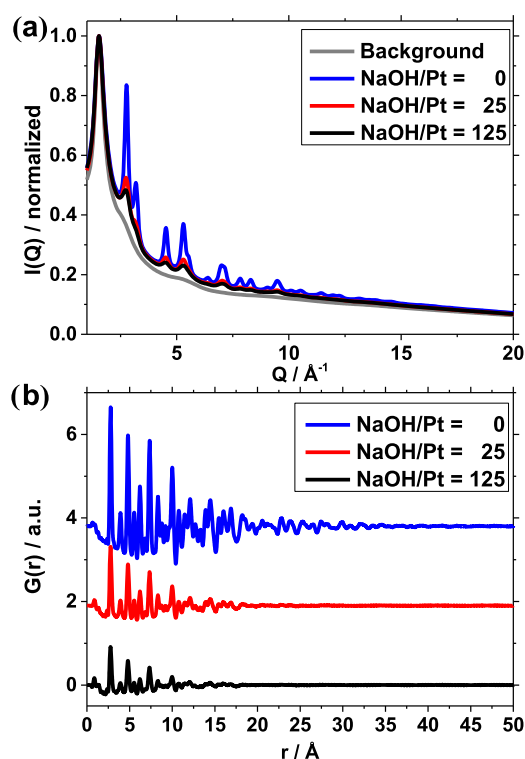

Figure 2. (a) Normalized intensity of X-ray total scattering data obtained for (b) PDF analysis of Pt nanoparticles prepared with different NaOH/Pt molar ratios of: (blue) 0, (red) 25, and (black) 125. An offset was added to the curves for display purposes.

structure (space group $Fd\bar{3}m$) and a spherical dampening function with a log−normal size distribution, as recently introduced in the characterization of zeolite-supported nanoparticles with PDF.[27] The fits obtained are shown in Figure 3 with the results summarized in Table 1. Fits using a single spherical dampening function, as usually applied in PDF modeling (Figure S1 and Table S1), underestimate the crystallite size and give large misfits to the PDF at higher r-values. This illustrates that modeling of the size distribution is
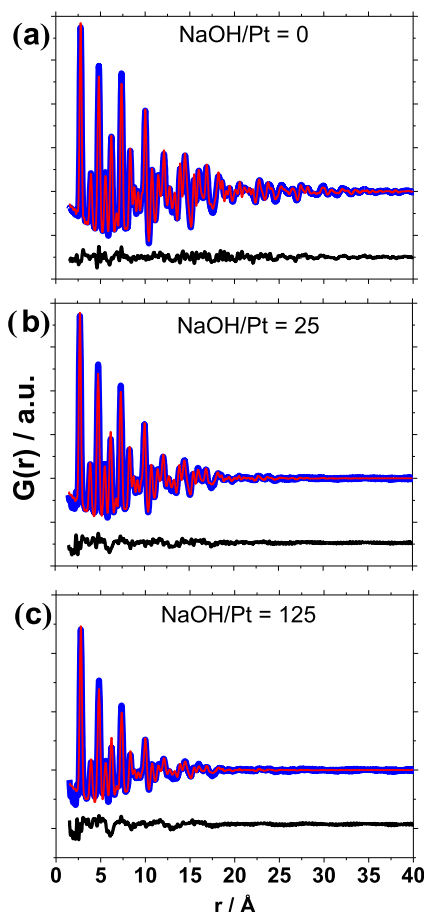
Figure 3. Raw data (blue), fit (red), and difference between fit and raw data (black) for Pt nanoparticles obtained with NaOH/Pt molar ratios of (a) 0, (b) 25, and (c) 125. The PDFs were modeled applying a log−normal distribution.
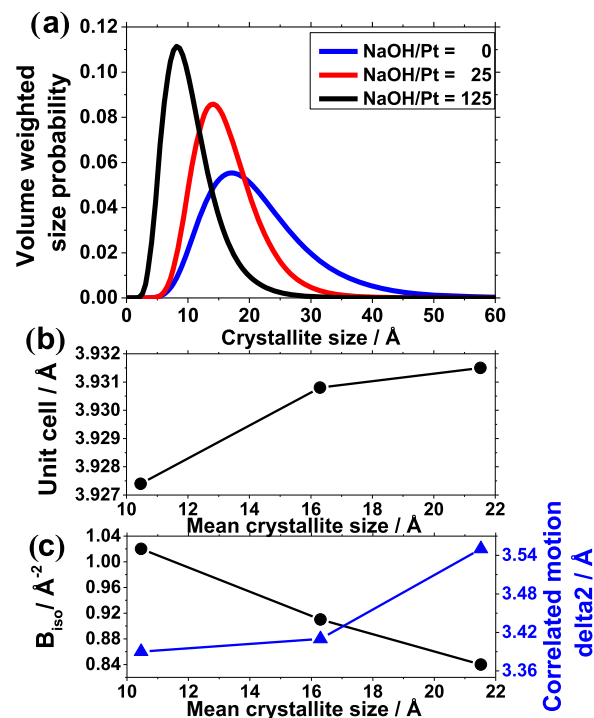

Figure 4. (a) Size distribution obtained from PDF analysis for Pt nanoparticles prepared with different NaOH/Pt molar ratios. (b) Unit cell as a function of mean crystallite size. (c) B_{iso} (left-hand axis) and correlated motion (delta2) parameters (right-hand axis) as a function of mean crystallite size.

particularly important in studies of very small nanoparticles (under 3 nm), where PDF is very sensitive to size.

The obtained size distributions are reported in Figure 4 and confirm that higher NaOH/Pt molar ratios lead to smaller nanoparticles. Overall, the refined size distributions are in agreement with the overall size determined by TEM, although the size determined from PDF is slightly smaller than what is observed from the TEM characterization for the nanoparticles in this study.

The fcc model agrees well with the data for all particle sizes. Since the pioneering work by Wang et al.[10] on the surfactant-free synthesis of Pt nanoparticles in EG, it is considered that

1−2 nm Pt nanoparticles have the fcc crystal structure as bulk Pt. X-ray scattering studies[28] and HRTEM[29] have further supported this observation. Here, it is successfully shown using PDF that even for the smallest nanoparticles obtained by the surfactant-free EG synthesis, the Pt nanoparticles crystallize in fcc structure and that size control of the nanocrystal domain can be achieved by controlling the NaOH/Pt molar ratio during synthesis. This result is in contrast to other metallic nanoparticles, for example, Ni and Pd, and Au, where nanosizing can dramatically change the atomic structure, and for example, icosahedral or decahedral motifs are seen.[14,15,30−33] Even though the fcc structure describes the main peaks for all samples, the fit quality decreases with decreasing crystallite size. This is often observed for nanoparticles where, for example, surface disorder is likely to be seen. In fcc nanoparticles, a similar misfit has previously been observed and assigned to structure rearrangements on the

Table 1. Table Comparing the Size of the Nanoparticles Obtained for Different NaOH/Pt Molar Ratios by UV-Induced Synthesis for PDF and TEM Analyzes

	PDF			TEM		
	log−normal distribution of spherical crystallites					
NaOH/Pt	0	25	125	0	25	125
mean size (diameter) (Å)	22	16	10	34	21	19
log−normal width of distribution (Å)	9	5	4	2	3	2
mode of the distribution (Å)	17	14	8	28	12	7
R_w (%)	11.2	12.6	18.4			
unit cell parameter a (Å)	3.932	3.931	3.927			
B_{iso} (Å^{-2})	0.84	0.91	1.02			
delta2 (correlated motion) (Å)	3.55	3.41	3.39			

surface.[14] The origin of the misfit may also be the presence of some degree of twining between crystalline domains in the nanoparticles. However, introducing known structures such as decahedra, icosahedra, or cube octahedra did not improve the fit quality.

The refined structural parameters are plotted as a function of mean size in Figure 4 and tabulated in Table 1. The unit cell parameter decreases with decreasing size, as also previously observed in Pt nanoparticles, where lattice contraction is known and believed to be related to surface effects.[24,25,34] We also see a clear effect of size on the B_{iso} values, which describes atomic motion in the Pt nanoparticles, but may also account for structural disorder. An increase in the B_{iso} parameter with decreasing particle size has previously been explained to arise from bond softening and disorder in carbon-supported Pt nanoparticles.[25] The delta2 parameter describes the correlated motion between neighboring atoms in the fcc structure, and again we see a clear trend, as the refined value decreases with decreasing size. The degree of correlated motion increases in the ordered, large particles.

When considering the PDFs at small r-values as shown in Figure S2, an additional small peak is present at 2.4 Å. This agrees well with a Pt−Cl distance, as previously observed in solutions of $H_2PtCl_6 \cdot 3H_2O$.[23] This indicates that a small amount of chloride is present in the sample, either present as $[PtCl_4]^{2-}$ complexes or as Cl^- coordinated to the surface of the Pt nanoparticles.

The UV-induced synthesis is a convenient synthesis method, which allows for well-controlled nucleation and growth of the nanoparticles, leading to narrow size distribution. As just demonstrated, size control is achieved for the nanocrystals by tuning the NaOH/Pt molar ratio. An additional and unique feature of UV synthesis is that it should also allow localized synthesis. Upon UV irradiation, the nanoparticles form only in the part of the solution exposed to UV irradiation. A proof-of-concept of such localized synthesis is presented in Figure 5a. It is demonstrated that Pt nanoparticles indeed only form in the

section of the cuvette not covered with aluminum foil. This demonstrates the potential for in situ localized formation of nanoparticles.

It is further established that the localized synthesis can be performed using a UV laser; see Figure 5b. Only on the area exposed to the UV light laser beam (spot of ca. 2 mm diameter at the cuvette interface as shown in the zoomed image), a brown color can be observed, which indicates the localized formation of Pt nanoparticles. With the nonfocused laser irradiation, the nanoparticle formation was limited to the interface. This could be due to the fact that the nanoparticles, once formed, can absorb the UV light and act as a filter. This leads to attenuation of the laser light, preventing the formation of nanoparticles further away from the surface. This phenomenon is often called the inner filter effect.[35] However, focusing or two-photon excitation should allow for depth control over the nanoparticle formation.[36]

CONCLUSIONS

In conclusion, it is shown by PDF characterization that the nanoparticles produced using UV light have an fcc crystal structure and that the size of the crystallite domains increases from 1.0 to 2.2 nm when the NaOH/Pt molar ratio decreases from 125 to 0. It is also demonstrated that UV-induced synthesis is promising to develop an in situ localized synthesis of Pt nanoparticles, for example, by focusing a UV beam on the reaction mixture. Structural information is essential to tailor the nanoparticles for specific needs, for example, in chemical synthesis or energy-related reactions. Further understanding of the nanoparticles formation could be gained by performing in situ PDF analysis during the nanoparticle synthesis. A deeper knowledge on the formation mechanism of the nanoparticles using for instance surfactants or different solvent mixtures could allow further control on the nanoparticle properties.

METHODS

UV-Induced Polyol Synthesis. The Pt nanoparticles were obtained using 2 mM $H_2PtCl_6 \cdot 6H_2O$ (99.9% Alfa Aesar) in alkaline NaOH (98.9%, Fisher Chemical) ethylene glycol (spectrophotometric grade, Alfa Aesar) with a NaOH/Pt molar ratio as indicated and for a volume of typically 3 mL. For UV-induced synthesis, the reaction mixture was placed in standard (10 mm path length) quartz cuvettes (capacity of 3.5 mL, 4.5 cm high) and placed in a home-built container equipped with 10 standard UV mercury lamps (PL-L 24 W/10/4P Hg, Philips) for 2 h. For localized synthesis of Pt nanoparticles, the UV-induced synthesis procedure with a NaOH/Pt molar ratio of ∼25 was used, but part of the cuvette was covered with aluminum foil. The irradiation time was 3 h. In contrast to a previous publication,[7] no temperature control was present during UV-induced synthesis of the Pt nanoparticles in this publication. Alternatively, a UV laser (375 nm, ∼0.9 mW, LDH-P-C-375, PicoQuant GmbH) was used with an exposure time of 2 h.

Nanoparticle Washing. Pt nanoparticles were collected and washed with 1 M aqueous solutions of HCl (prepared from 30% HCl Suprapur, EMD Millipore, Merck KGaA in ultrapure water, Milli-Q, Millipore, 18.2 MΩ·cm) in a volume ratio of around 1:3. The dark precipitate was centrifuged at 2400 relative centrifugal force (4000 rpm, Sigma 2−5 laboratory centrifuge, Sigma-Aldrich) for 5 min. This washing
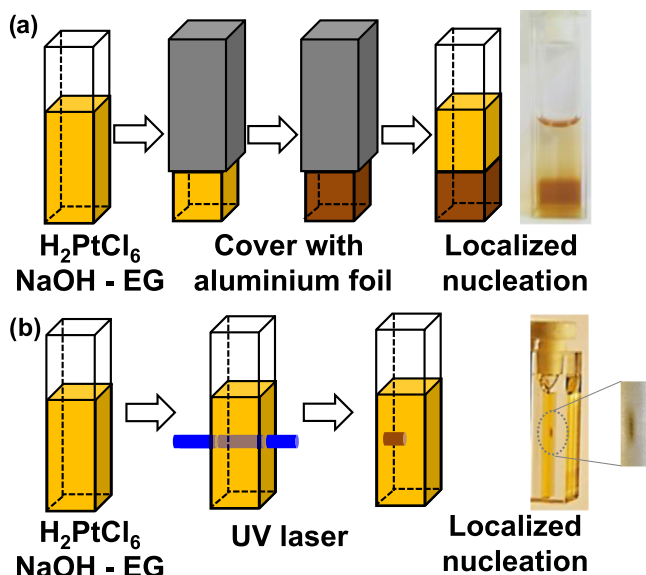

(a) H₂PtCl₆ NaOH - EG → Cover with aluminium foil → Localized nucleation

(b) H₂PtCl₆ NaOH - EG → UV laser → Localized nucleation

Figure 5. (a, b) Schematic representation and pictures of localized synthesis of Pt nanoparticles obtained using UV-induced synthesis. Large-scale pictures of the cuvettes are provided in Figure S3 in the Supplementary Information.

step was repeated twice to remove any remaining EG or NaOH.

TEM Characterization. For TEM analysis, a Jeol 2100 microscope operated at 200 kV was used. For TEM, the Pt nanoparticles were washed and redispersed in pure ethanol (99.9%, Kemetyl) and diluted 50 times as previously described.[7] Small drops of colloids then were placed on carbon-coated copper grids (300 mesh grids, Quantifoil) and dried in room conditions. The size and size distribution analyzes were performed by measuring the size of typically 200 (at least 165) nanoparticles with ImageJ software, and samples were characterized by taking images of (at least) three different magnifications in (at least) five different areas of the TEM grids. The log−normal distribution parameters were obtained using the fit function of OriginPro software on the relevant data set.

X-ray Total Scattering Data Collection and PDF Analysis. X-ray total scattering data were collected at beamline P02.1, PETRAIII, DESY. The data were collected with an X-ray wavelength of 0.2072 Å, using the PerkinElmer detector (200 by 200 μm pixel size) at a detector distance of 20.059 cm. The samples were loaded in 1 mm Kapton tubes. Prior to the measurements, the nanoparticles were washed in HCl as described above and redispersed in EG to obtain a concentration of Pt ca. 140 mM for the measurements. EG was used as background. Data were collected for each sample for 12 min. The data were integrated using Fit2D,[37] Fourier transformed in xPDFsuite,[38,39] and modeled using Diffpy-CMI.[26]

ASSOCIATED CONTENT

Ⓢ Supporting Information

The Supporting Information is available free of charge on the ACS Publications website at DOI: 10.1021/acsomega.8b01613.

PDF data, picture of nanoparticles obtained by UV-laser-induced synthesis (PDF)

AUTHOR INFORMATION

Corresponding Authors
*E-mail: jonathan.quinson@chem.ku.dk (J.Q.).
*E-mail: tom@chem.ku.dk (T.V.).
*E-mail: matthias.arenz@dcb.unibe.ch (M.A.).
*E-mail: kirsten@chem.ku.dk (K.M.Ø.J.).

ORCID Ⓞ
Jonathan Quinson: 0000-0002-9374-9330
Tom Vosch: 0000-0001-5435-2181
Matthias Arenz: 0000-0001-9765-4315

Author Contributions
§J.Q. and L.K. contributed equally to this work.

Author Contributions
The manuscript was written through contributions of all authors. All authors have given approval to the final version of the manuscript.

Notes
The authors declare no competing financial interest.

REFERENCES

(1) Olveira, S.; Forster, S. P.; Seeger, S. Nanocatalysis: academic discipline and industrial realities. *J. Nanotechnol.* **2014**, No. 324089.

(2) Antolini, E. Structural parameters of supported fuel cell catalysts: the effect of particle size, inter-particle distance and metal loading on catalytic activity and fuel cell performance. *Appl. Catal., B* **2016**, *181*, 298−313.

(3) Quinson, J.; Inaba, M.; Neumann, S.; Swane, A.; Bucher, J.; Simonsen, S.; Theil Kuhn, L.; Kirkensgaard, J.; Jensen, K.; Oezaslan, M.; Kunz, S.; Arenz, M. Investigating particle size effects in catalysis by applying a size-controlled and surfactant-free synthesis of colloidal nanoparticles in alkaline ethylene glycol: case study of the oxygen reduction reaction on Pt. *ACS Catal.* **2018**, *8*, 6627−6635.

(4) Nørskov, J. K.; Rossmeisl, J.; Logadottir, A.; Lindqvist, L.; Kitchin, J. R.; Bligaard, T.; Jonsson, H. Origin of the overpotential for oxygen reduction at a fuel-cell cathode. *J. Phys. Chem. B* **2004**, *108*, 17886−17892.

(5) Sun, Y.; Zhuang, L.; Lu, J.; Hong, X.; Liu, P. Collapse in crystalline structure and decline in catalytic activity of Pt nanoparticles on reducing particle size to 1 nm. *J. Am. Chem. Soc.* **2007**, *129*, 15465.

(6) Billinge, S. J. L.; Levin, I. The problem with determining atomic structure at the nanoscale. *Science* **2007**, *316*, 561−565.

(7) Kacenauskaite, L.; Quinson, J.; Schultz, H.; Kirkensgaard, J. J. K.; Kunz, S.; Vosch, T.; Arenz, M. UV-induced synthesis and stabilization of surfactant-free colloidal Pt nanoparticles with controlled particle size in ethylene glycol. *ChemNanoMat* **2017**, *2*, 89−93.

(8) Dong, H.; Chen, Y. C.; Feldmann, C. Polyol synthesis of nanoparticles: status and options regarding metals, oxides, chalcogenides, and non-metal elements. *Green Chem.* **2015**, *17*, 4107−4132.

(9) Fiévet, F.; Ammar-Merah, S.; Brayner, R.; Chau, F.; Giraud, M.; Mammeri, F.; Peron, J.; Piquemal, J.-Y.; Sicarda, L.; Viaub, G. The polyol process: a unique method for easy access to metal nanoparticles with tailored sizes, shapes and compositions. *Chem. Soc. Rev.* **2018**, 5187.

(10) Wang, Y.; Ren, J. W.; Deng, K.; Gui, L. L.; Tang, Y. Q. Preparation of tractable platinum, rhodium, and ruthenium nanoclusters with small particle size in organic media. *Chem. Mater.* **2000**, *12*, 1622−1627.

(11) Kacenauskaite, L.; Swane, A. A.; Kirkensgaard, J. J. K.; Fleige, M.; Kunz, S.; Vosch, T.; Arenz, M. Synthesis mechanism and influence of light on unprotected platinum nanoparticles synthesis at room temperature. *ChemNanoMat* **2016**, *2*, 104−107.

(12) Inaba, M.; Quinson, J.; Arenz, M. pH matters: The influence of the catalyst ink on the oxygen reduction activity determined in thin film rotating disk electrode measurements. *J. Power Sources* **2017**, *353*, 19−27.

(13) Jin, R. Quantum sized, thiolate-protected gold nanoclusters. *Nanoscale* **2010**, *2*, 343−362.

(14) Doan-Nguyen, V. V. T.; Kimber, S. A. J.; Pontoni, D.; Hickey, D. R.; Diroll, B. T.; Yang, X. H.; Miglierini, M.; Murray, C. B.; Billinge, S. J. L. Bulk metallic glass-like scattering signal in small metallic nanoparticles. *ACS Nano* **2014**, *8*, 6163−6170.

(15) Jensen, K. M. Ø.; Juhas, P.; Tofanelli, M. A.; Heinecke, C. L.; Vaughan, G.; Ackerson, C. J.; Billinge, S. J. L. Polymorphism in magic-sized Au144(SR)60 clusters. *Nat. Commun.* **2016**, *7*, No. 11859.

(16) Billinge, S. J. L.; Kanatzidis, M. G. Beyond crystallography: the study of disorder, nanocrystallinity and crystallographically challenged materials with pair distribution functions. *ChemComm* **2004**, 749−760.

(17) Paglia, G.; Bozin, E. S.; Billinge, S. J. L. Fine-scale nanostructure in gamma-Al_2O_3. *Chem. Mater.* **2006**, *18*, 3242−3248.

(18) Masadeh, A. S.; Bozin, E. S.; Farrow, C. L.; Paglia, G.; Juhas, P.; Billinge, S. J. L.; Karkamkar, A.; Kanatzidis, M. G. Quantitative size-dependent structure and strain determination of CdSe nanoparticles using atomic pair distribution function analysis. *Phys. Rev. B* **2007**, *76*, No. 115413.

(19) Yang, X.; Masadeh, A. S.; McBride, J. R.; Bozin, E. S.; Rosenthal, S. J.; Billinge, S. J. L. Confirmation of disordered structure of ultrasmall CdSe nanoparticles from X-ray atomic pair distribution function analysis. *Phys. Chem. Chem. Phys.* **2013**, *15*, 8480−8486.

(20) Newton, M. A.; Chapman, K. W.; Thompsett, D.; Chupas, P. J. Chasing changing nanoparticles with time-resolved pair distribution function methods. *J. Am. Chem. Soc.* **2012**, *134*, 5036−5039.

(21) Chupas, P. J.; Chapman, K. W.; Jennings, G.; Lee, P. L.; Grey, C. P. Watching nanoparticles grow: the mechanism and kinetics for the formation of TiO_2-supported platinum nanoparticles. *J. Am. Chem. Soc.* **2007**, *129*, 13822−13824.

(22) Jacques, S. D. M.; Di Michiel, M.; Kimber, S. aJ.; Yang, X.; Cernik, R. J.; Beale, A. M.; Billinge, S. J. L. Pair distribution function computed tomography. *Nat. Commun.* **2013**, *4*, No. 2536.

(23) Saha, D.; Bojesen, E. D.; Jensen, K. M. O.; Dippel, A. C.; Iversen, B. B. Formation mechanisms of Pt and Pt_3Gd nanoparticles under solvothermal conditions: an in situtotal X-ray scattering study. *J. Phys. Chem. C* **2015**, *119*, 13357−13362.

(24) Lei, Y.; Zhao, H. Y.; Rivas, R. D.; Lee, S.; Liu, B.; Lu, J. L.; Stach, E.; Winans, R. E.; Chapman, K. W.; Greeley, J. P.; Miller, J. T.; Chupas, P. J.; Elam, J. W. Adsorbate-induced structural changes in 1−3 nm platinum nanoparticles. *J. Am. Chem. Soc.* **2014**, *136*, 9320−9326.

(25) Shi, C. Y.; Redmond, E. L.; Mazaheripour, A.; Juhas, P.; Fuller, T. F.; Billinge, S. J. L. Evidence for anomalous bond softening and disorder below 2 nm diameter in carbon-supported platinum nanoparticles from the temperature-dependent peak width of the atomic pair distribution function. *J. Phys. Chem. C* **2013**, *117*, 7226−7230.

(26) Juhás, P.; Farrow, C. L.; Yang, X. H.; Knox, K. R.; Billinge, S. J. L. Complex modeling: a strategy and software program for combining multiple information sources to solve ill posed structure and nanostructure inverse problems. *Acta Crystallogr., Sect. A: Found. Adv.* **2015**, *71*, 562−568.

(27) Gamez-Mendoza, L.; Terban, M. W.; Billinge, S. J. L.; Martinez-Inesta, M. Modelling and validation of particle size distributions of supported nanoparticles using the pair distribution function technique. *J. Appl. Crystallogr.* **2017**, *50*, 741−748.

(28) Bock, C.; Paquet, C.; Couillard, M.; Botton, G. A.; MacDougall, B. R. Size-selected synthesis of PtRu nano-catalysts: Reaction and size control mechanism. *J. Am. Chem. Soc.* **2004**, *126*, 8028−8037.

(29) Baranova, E. A.; Bock, C.; Ilin, D.; Wang, D.; MacDougall, B. Infrared spectroscopy on size-controlled synthesized Pt-based nano-catalysts. *Surf. Sci.* **2006**, *600*, 3502−3511.

(30) Kwon, K.; Lee, K. Y.; Lee, Y. W.; Kim, M.; Heo, J.; Ahn, S. J.; Han, S. W. Controlled synthesis of icosahedral gold nanoparticles and their surface-enhanced Raman scattering property. *J. Phys. Chem. C* **2007**, *111*, 1161−1165.

(31) Daniel, M. C.; Astruc, D. Gold nanoparticles: Assembly, supramolecular chemistry, quantum-size-related properties, and applications toward biology, catalysis, and nanotechnology. *Chem. Rev.* **2004**, *104*, 293−346.

(32) Jin, R.; Zhu, Y.; Qian, H. Quantum-sized gold nanoclusters: bridging the gap between organometallics and nanocrystals. *Chem. -Eur. J.* **2011**, *17*, 6584−6593.

(33) Negishi, Y.; Nakazaki, T.; Maloa, S.; Takano, S.; Niihori, Y.; Kurashige, W.; Yamazoe, S.; Tsukuda, T.; Hakkinen, H. A critical size for emergence of nonbulk electronic and geometric structures in dodecanethiolate-protected Au clusters. *J. Am. Chem. Soc.* **2015**, *137*, 1206−1212.

(34) Leontyev, I. N.; Kuriganova, A. B.; Leontyev, N. G.; Hennet, L.; Rakhmatullin, A.; Smirnova, N. V.; Dmitriev, V. Size dependence of the lattice parameters of carbon supported platinum nanoparticles: X-ray diffraction analysis and theoretical considerations. *RSC Adv.* **2014**, *4*, 35959−35965.

(35) Lakowicz, J. R. *Principles of Fluorescence Spectroscopy*, 3rd ed.; Springer, 2006.

(36) De Cremer, G.; Sels, B. F.; Hotta, J.; Roeffaers, M. B. J.; Bartholomeeusen, E.; Coutino-Gonzalez, E.; Valtchev, V.; De Vos, D. E.; Vosch, T.; Hofkens, J. Optical encoding of silver zeolite microcarriers. *Adv. Mater.* **2010**, *22*, 957.

(37) Hammersley, A. P.; Svensson, S. O.; Hanfland, M.; Fitch, A. N.; Hausermann, D. Two-dimensional detector software: from real detector to idealised image or two-theta scan. *High Pressure Res.* **1996**, *14*, 235−248.

(38) Yang, X.; Juhas, P.; Farrow, C. L.; Billinge, S. J. L. xPDFsuite: an end-to-end software solution for high throughput pair distribution function transformation, visualization and analysis, arXiv:1402.3163, arXiv.org e-Print archive. https://arxiv.org/abs/1402.3163, 2015.

(39) Juhás, P.; Davis, T.; Farrow, C. L.; Billinge, S. J. L. PDFgetX3: a rapid and highly automatable program for processing powder diffraction data into total scattering pair distribution functions. *J. Appl. Crystallogr.* **2013**, *46*, 560−566.